



# Multifunctional Lightweight Mortars for Indoor Applications to Improve Comfort and Health of Occupants: Thermal Properties and Photocatalytic Efficiency

Chiara Giosuè<sup>1\*</sup>, Mattia Pierpaoli<sup>2</sup>, Alessandra Mobili<sup>1</sup>, Maria Letizia Ruello<sup>1</sup> and Francesca Tittarelli<sup>1,3\*</sup>

<sup>1</sup> Department of Materials, Environmental Sciences and Urban Planning (SIMAU), Università Politecnica delle Marche – INSTM Research Unit, Ancona, Italy, <sup>2</sup> Faculty of Electronics, Telecommunications and Informatics, Gdańsk University of Technology, Gdańsk, Poland, <sup>3</sup> Institute of Atmospheric Sciences and Climate, National Research Council (ISAC-CNR), Bologna, Italy

## OPEN ACCESS

### Edited by:

Emilia Morallon,  
University of Alicante, Spain

### Reviewed by:

Maria Angeles Lillo-Rodenas,  
University of Alicante, Spain

Inês Flores-Colen,  
Instituto Superior Técnico, Portugal

Mohammed Ouzzine,  
Université Sultan Moulay Slimane,  
Morocco

### \*Correspondence:

Chiara Giosuè  
c.giosue@univpm.it  
Francesca Tittarelli  
f.tittarelli@univpm.it

### Specialty section:

This article was submitted to  
Ceramics and Glass,  
a section of the journal  
Frontiers in Materials

**Received:** 11 May 2020

**Accepted:** 14 July 2020

**Published:** 26 August 2020

### Citation:

Giosuè C, Pierpaoli M, Mobili A,  
Ruello ML and Tittarelli F (2020)  
Multifunctional Lightweight Mortars  
for Indoor Applications to Improve  
Comfort and Health of Occupants:  
Thermal Properties and Photocatalytic  
Efficiency. *Front. Mater.* 7:255.  
doi: 10.3389/fmats.2020.00255

A new generation of smart building materials, able to passively improve the indoor environment and the comfort of occupants owing to their interaction with the surrounding environment, can be addressed. This paper investigates the use of three highly porous aggregates to manufacture hydraulic lime-based multifunctional mortars to be used as indoor finishes. The same water/binder ratio was used for each mortar mix, and conventional calcareous sand was totally replaced by volume with zeolite, silica gel, and activated carbon. Nanosized titanium dioxide (TiO<sub>2</sub>) was added to award a photocatalytic behavior under UV radiation to the mortars. Results show that, as expected, when highly porous aggregates are used, mortars absorb more water by capillary suction. However, even though the mortars manufactured with lightweight aggregates have a lower density, the mechanical behavior of zeolite and activated carbon mortars is comparable or even higher than that of sand mortars, thanks to an optimum interfacial transition zone (ITZ) between the binder paste and the aggregate. The photocatalytic activity, in terms of photocatalytic NO<sub>x</sub> degradation efficiency and selectivity of unwanted produced NO<sub>2</sub>, results to be optimal when silica gel-based mortar is tested. Additionally, the thermal-insulation properties are enhanced up to 40% by using all the unconventional aggregates.

**Keywords:** Indoor Air Quality, lightweight mortar, titanium dioxide photocatalytic oxidation, capillary water absorption, thermal conductivity

## INTRODUCTION

A remarkable issue of modern time is the sustainability of the building sector since it contributes 40% on global carbon dioxide emissions (Wang et al., 2012). For this reason, nowadays European laws and directives are becoming stricter in terms of energy efficiency and, consequentially, more sealed buildings are assembled and not enough air changing can be guaranteed (Wolkoff, 2013). In this condition, the concentration of chemical, physical, and biological pollutants, such as volatile

organic compounds (VOCs), anhydrides, particulate matters, and molds, can be higher inside than outside, impairing the Indoor Air Quality (IAQ) of living environments. Currently, people are spending about 90% of their time indoor (Frey et al., 2015); thus, it is of utmost importance that the indoor living environment is wholesome to guarantee the health and comfort of occupants (Pierpaoli and Ruello, 2018).

Several strategies are used to improve the IAQ also in terms of thermal comfort; the conventional ones are source control, dilution by ventilation, and active engineered control systems (in heating, ventilation, and air-conditioning, HVAC) or stand-alone air purifiers (Matsumoto et al., 2009). Active control systems are generally more effective than passive systems for the control of IAQ, but they have a substantial energy loss that can be reduced by the addition of passive systems in the environment (Trník et al., 2016). Moreover, the combination of multiple techniques to improve IAQ, and in particular to remove pollutants, may result in a more efficient synergistic effect than the sum of the individual ones (Pierpaoli et al., 2017, 2019a). To remove pollutants, titanium dioxide ( $\text{TiO}_2$ ) is the most studied photocatalytic agent, because of its chemical inertness, non-toxicity, and low cost. Therefore, there is an increasing interest in using such catalyst in cementitious materials (Ballari et al., 2011; Folli et al., 2012).

Smart materials are based on the innovative concept of designing the material composition by introducing functional components into the matrix (Han et al., 2016) able to give different functionalities to the same material such as good mechanical performances, lightness, and ability to improve IAQ in terms of low thermal conductivity, to act as an hygroscopic buffer (Senff et al., 2018), and/or to remove pollutants.

In this case, the addition of highly porous materials with adsorbent properties is the key aspect to providing the multifunctionality of mortars, as successfully demonstrated in previous works where they were added to commercial finishes (Giosuè et al., 2017a). Several studies have tested the  $\text{NO}_x$  photocatalytic degradation, where  $\text{TiO}_2$ , added at 1–4% by binder mass, gives a removal efficiency ranging from 30 to 80% (Senff et al., 2013, 2018), also under visible irradiation (Giosuè et al., 2018).




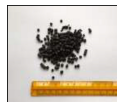
In the current study, the photocatalytic activity is associated with the adsorption of unconventional highly porous aggregates added to different mixes. The adsorption on a solid surface can be influenced by forces of electrostatic nature due to differences in polarity and differences in molecular weight and molecular geometry which induce selective deposition on the solid surface (Masel, 1996). The adsorption process is preferred on solids with a high specific surface since adsorption is a superficial process (Matsumoto et al., 2009). In mortars, the effectiveness of adsorbent aggregates to remove VOCs can reach 65%, as it has been previously tested (Tittarelli et al., 2015; Giosuè et al., 2019b). Adsorbent fillers/aggregates have been also tested to remove  $\text{NO}_x$  in cementitious systems with photocatalytic agents under UV-A radiation (Horgnies et al., 2012; Pierpaoli et al., 2019b).

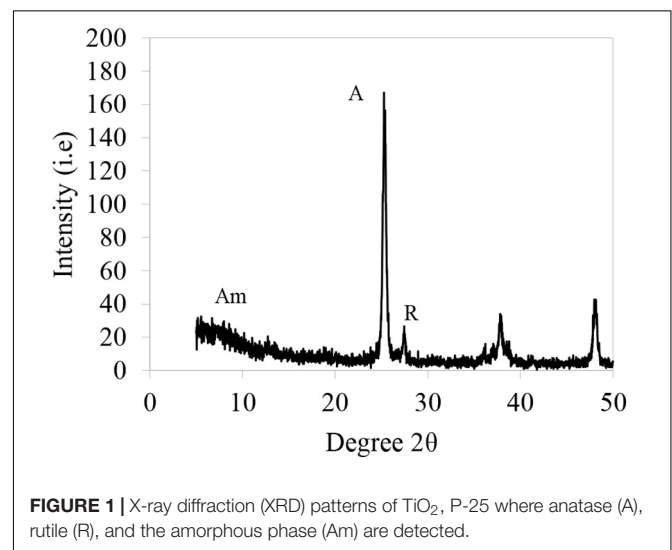
The use of unconventional highly porous aggregates can also be employed to develop lightweight mortars with low sound transmission (Branco and Godinho, 2013) and minimal thermal

transmittance (Benfratello et al., 2013; Branco and Godinho, 2013; Giosuè et al., 2019b) to the advantage of thermal efficiency and indoor sound comfort. It is well known that thermal conductivity can be reduced by the addition of aggregates with low bulk density and/or low thermal conductivity (Benfratello et al., 2013). Another positive effect is the reduction of the material density with a consequent lowering of dead loads on the structure. Nevertheless, in materials the reduction of density is often related to the reduction in compressive strength (Demirboga and Gül, 2003; Yu et al., 2015).

The current work is aimed to develop innovative multifunctional mortars for indoor finishes/renderers able to passively improve IAQ, besides fulfilling the ordinary requirements (according to the standard EN 998). The main objective is not to find the mortar with the best

**TABLE 1** | Properties of different aggregates.

Mix	Image	ID	Density $\text{kg/m}^3$	Water absorption %
Calcareous sand		S	2650	5
Zeolite		A1	1600	20
Silica gel		A2	1310	86
Activated carbon		A3	530	30



**TABLE 2** | Mix proportions (g/L), density (kg/m<sup>3</sup>), and accessible total porosity (%) of mortars.

Mix	Mix proportions							Density kg/m <sup>3</sup>	Accessible porosity %
	Water	HL	S	A1	A2	A3	TiO <sub>2</sub>		
M0-S	255	440	1535	–	–	–	–	1800	32
M0-S TiO <sub>2</sub>	255	414	1535	–	–	–	26		
M1-A1	255	440	–	927	–	–	–	1390	41
M1-A1 TiO <sub>2</sub>	255	414	–	927	–	–	26		
M2-A2	255	440	–	–	759	–	–	910	47
M2-A2 TiO <sub>2</sub>	255	414	–	–	759	–	26		
M3-A3	255	440	–	–	–	683	–	1210	35
M3-A3 TiO <sub>2</sub>	255	414	–	–	–	683	26		

mechanical properties, but to compare mortars that can act as multifunctional renders/finishes being able to improve also IAQ.

For this purpose, hydraulic lime is used as binder with and without the addition of TiO<sub>2</sub>. Lime-based mortars are extensively used as renders/plasters in indoor applications. Moreover, hydraulic lime mortars are commonly used for rehabilitation of historical buildings where cement-based mortars are not allowed, and lime is a more sustainable binder than ordinary Portland cement (Barcelo et al., 2013; Lucas et al., 2013). It has been also demonstrated that hydraulic lime provides to mortars a higher depolluting activity than cement; this is due not only for the lower presence of mineralogical components that can hide the catalyst (Sugrañez et al., 2013; Kaja et al., 2019) but also for the higher porosity of its hardened microstructure (Karatasios et al., 2010; Giosuè et al., 2018).

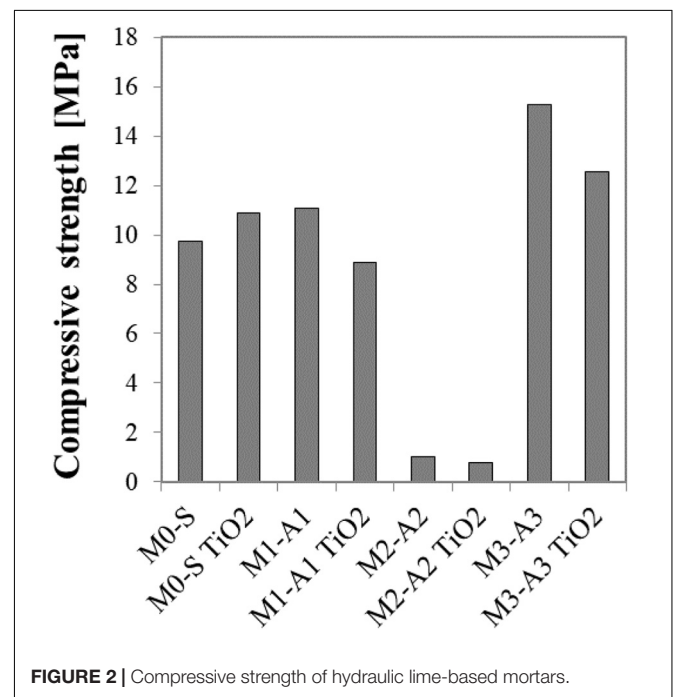
The conventional sand is substituted by highly porous and adsorbent materials usually employed in filters for water–air cleaning processes as zeolite, silica gel, and activated carbon. As reference, a conventional sand-based mortar is used.

The mechanical strength and porosity of these mortars have been measured in a previous work (Giosuè et al., 2020). Here, the different compressive strength values are correlated with the corresponding microstructures observed by scanning electronic microscopy (SEM). Moreover, the behavior under capillary water absorption is investigated. In order to find the best mortar for improving the indoor comfort and health of indoor occupants, the corresponding thermal conductivity and photocatalytic activity are also tested. The previous work has demonstrated the optimum hygroscopic behavior of these mortars in terms of moisture buffering capacity and water vapor permeability but also a photocatalytic activity hidden by the adsorption process until saturation of specimens (Giosuè et al., 2020). Therefore, in this paper, to demonstrate the effectiveness of photocatalytic activity in batch, all mortars are tested in saturated conditions.

## MATERIALS AND METHODS

### Materials

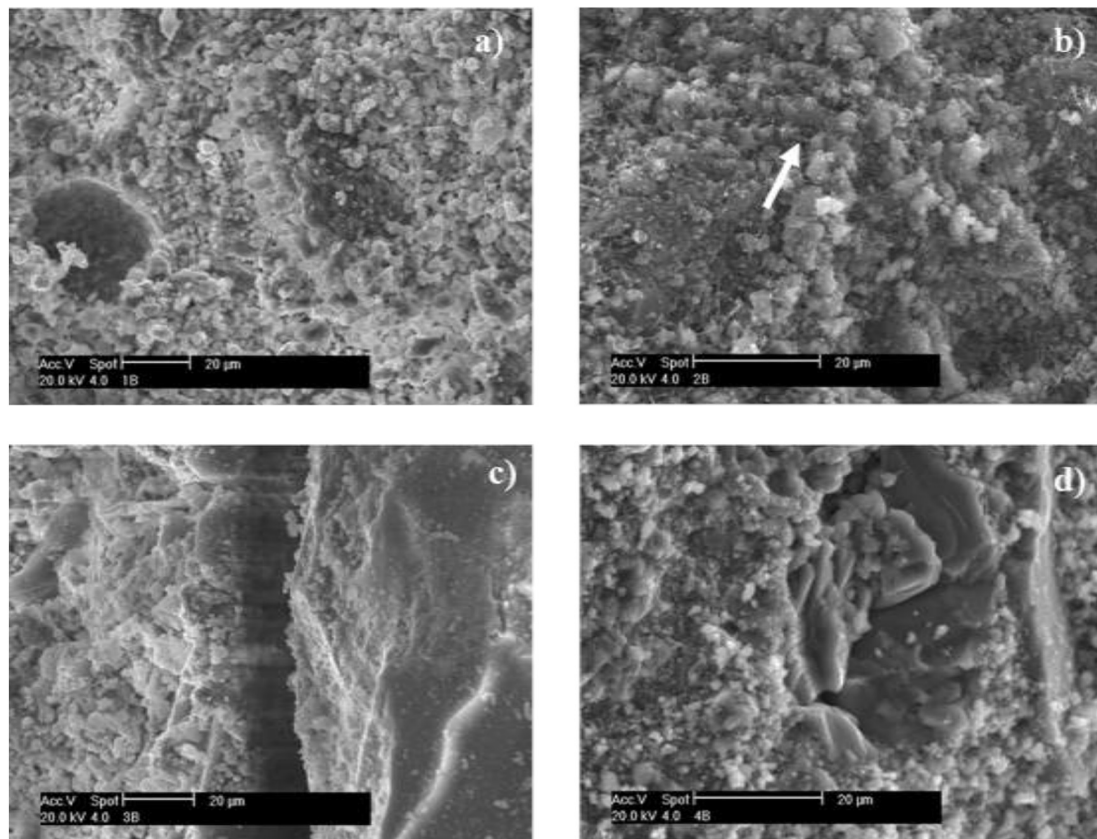
The binder is a commercial hydraulic lime LIC 3.0, according to UNI EN 15368, with a density of 2650 kg/m<sup>3</sup>. As aggregates, sand

**FIGURE 2** | Compressive strength of hydraulic lime-based mortars.

(S) is fully substituted by volume with selected unconventional aggregates, namely, natural clinoptilolite zeolite (A1), silica gel (A2), and activated carbon (A3). During the cast, all aggregates are added in saturate surface dry (SSD) condition, which means that all voids of aggregates are saturated by water but the surface is dry; hence, when the water necessary for the cast is added, no water exchange between the aggregate and the paste takes place. The density and water absorption of all aggregates to reach the SSD condition are evaluated and summarized in **Table 1**.

A commercially available titanium dioxide, TiO<sub>2</sub>, P-25 Aeroxide by Evonik, is used as photocatalytic agent, added by replacing 5% of the binder weight. TiO<sub>2</sub>, in powder form, was added to the dry cement mixture prior to the water addition, carefully mixed manually for 3 min and then with a mortar mixer.

As reported in the data sheet, its chemical composition is a mixture of anatase–rutile–amorphous phases, 78–14–8% in weight, respectively. Particles have nano-size dimension around 20–50 nm. The specific surface, measured by BET, is 35–65 m<sup>2</sup>/g,



**FIGURE 3** | SEM images of mortars manufactured with different aggregates and TiO<sub>2</sub>. **(a)** HL-S TiO<sub>2</sub>, **(b)** HL-A1 TiO<sub>2</sub>, **(c)** HL-A2 TiO<sub>2</sub>, **(d)** HL-A3 TiO<sub>2</sub>.

and density is equal to 3100 kg/m<sup>3</sup>. The pH value of 4% dispersion in water is 3.5–4.5. The X-ray diffraction (XRD) pattern is shown in **Figure 1** where the crystalline phases are detected.

The mixes are prepared by keeping constant the water to binder ratio at 0.6. Mix proportions, density, and accessible total porosity of cured mortars without TiO<sub>2</sub> (since these properties were not significantly affected by TiO<sub>2</sub> nanoparticles) are reported in **Table 2** (Giosuè et al., 2020).

Since the retail price in Euro/kg is about 0.10 for calcareous sand, 2.02 for zeolite, 0.59 for silica gel, 5.00 for activated carbon, 44 for TiO<sub>2</sub>, and 0.14 for HL, the price in Euro/m<sup>3</sup> of the photocatalytic mortars with zeolite and activated carbon is about double that with conventional sand, whereas the price in Euro/m<sup>3</sup> of the silica gel photocatalytic mortar is about half that of conventional sand photocatalytic mortar.

## Methods

Mortars are casted and then cured for 28 days according to the UNI EN 1015-11 procedure: at temperature (*T*) of 20°C and relative humidity (RH) of 95% for 7 days and then at 20°C *T* and 65% RH. After 28 days of curing, mortars are tested according to the current standards.

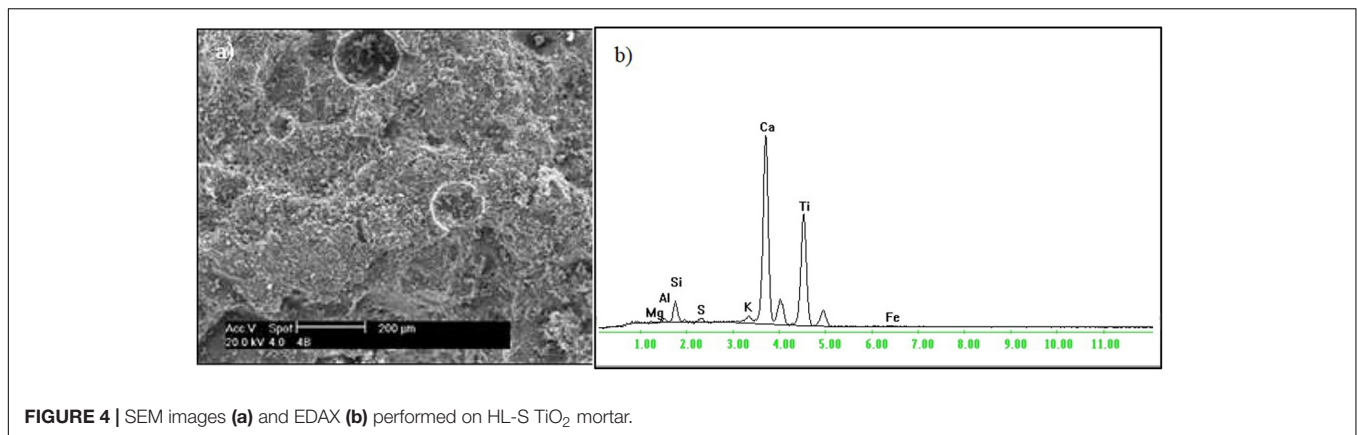
Properties such as mechanical performance, density, and porosity of these mortars have been already investigated in

Giosuè et al. (2020) and are briefly summarized in the current paper. Compressive strength is measured by means of a hydraulic press (Galdabini) after 28 days of curing. Density is evaluated by the ratio between the weight of the specimen and its dimension, measured with a caliper. Each measurement is repeated three times, and the average values are reported. The dry weight is evaluated after placing the specimens in oven at *T* = 105°C until a constant weight is reached (when the change in the weight of the test specimen over 24 h period is less than 0.1%). Porosity is evaluated by means of MIP (Thermo Fisher, Pascal series 240) on samples after 28 days of curing on three fragments per mortar of 1 cm<sup>3</sup> volume, and the average results are reported.

In this study, the mechanical strengths are correlated with the microstructures observed by SEM. Moreover, the capillary water absorption, the photocatalytic behavior by NO<sub>x</sub> degradation test, and thermal conductivity are further investigated.

The morphology is analyzed by means of the SEM ZEISS 1530 (Carl Zeiss, Oberkochen, Germany) equipped with a Schottky emitter, with two different secondary electrons detectors (the in-lens and the Everhart-Thornley) and operating at 10 keV (EDAX probe). Specimens are fragments of about 1 cm<sup>3</sup>.

Capillary water absorption is investigated according to UNI EN 15801. Capillary water absorption is affected not only by the pores volume but also by the distribution and size of the pores, since the lower the pore diameter, the higher the level



reached by the rising water, according to the Washburn's equation (Washburn, 1921). Test specimens are prisms 160 × 40 × 40 mm broken in two halves. Specimens are dried in an oven at 105°C until the constant mass is reached (difference in the weight values measured after 24 h should be lower than 0.1%). The specimens are placed on a water-saturated filter paper, and the capillary water absorbed by the tested surface (16 cm<sup>2</sup>) is monitored over time by weighing the specimens periodically. The results are expressed as water absorbed per unit area  $Q_i$  (kg/m<sup>2</sup>) at time  $t_i$  (s<sup>0.5</sup>).

Concerning photocatalytic efficiency, after curing, the pH of mortars is measured in order to demonstrate the lowering of the basicity of the mixes. It is well known that CO<sub>2</sub> can penetrate within the matrix as easily as the porosity increases, interacting with the matrix through the carbonation process. This process causes the decrease of the pH and the densification of the matrix owing to the precipitation of calcite. In turn, calcite can cause the occlusion of the catalysts (Sugrañez et al., 2013). Also, the redox process that occurs at the TiO<sub>2</sub> surface is influenced by the pH, due to the Nernst relationship (MacPhee and Folli, 2016). 1 g of material is collected on a glass slide; then, a drop of water (about 1 ml) is added and the pH of the solution is measured.

The test adopted for assessing the photocatalytic property of the mortars follows the UNI 11247 procedure, which assesses the photocatalytic activity of inorganic photocatalytic materials by determining the degradation rate of nitrogen oxides (NO<sub>x</sub>) in air. Therefore, the NO<sub>x</sub> photocatalytic activity is expressed by the ratio of removed NO<sub>x</sub> over total NO<sub>x</sub> flux under plug flow conditions. Briefly, a NO<sub>x</sub> flux is directed inside the reactor by a NO<sub>x</sub> tank, 499 ppb NO (SAPIO S.r.l., Monza, Italy), and it is kept constant with a dilution system (Calibrator 8188, Rancon Instruments S.p.A., Milan, Italy) by mixing with atmospheric air at  $T = 25 \pm 2^\circ\text{C}$  and RH between 40 and 50%. NO and NO<sub>2</sub> concentrations are continuously monitored by a chemiluminescence NO<sub>x</sub> analyzer (nitrogen oxide analyzer model 8841, Monitor Labs, Englewood, CO, United States) at the reactor outlet. The photoreactor consists of a 3-L borosilicate glass cylinder, in the center of which the specimens (8 cm diameter and 0.8 cm height) are placed. A UV metal halogen lamp, having a measured irradiance of 20 W/m<sup>2</sup>, is placed outside the reactor over the specimen and placed at 25 cm from the

specimen' surface. The irradiation of the sample is guaranteed until stable conditions are reached, usually 30 min.

The thermal conductivity ( $\lambda$ , in W/mK) of specimens is measured at room temperature ( $T = 20^\circ\text{C}$ ) and RH = 50%. Specimens are cylinders of 14 cm diameter and 3 cm height. The test is performed according to the UNI EN 12664 standard and  $\lambda$  calculated by the following equation (Eq. 1):

$$\lambda = \frac{Jd}{(T_1 - T_2)} \quad (1)$$

where  $J$  is the heat flux (W/m<sup>2</sup>),  $d$  is the distance between thermocouples (m), and  $T_1$  and  $T_2$  are the temperatures at the two different sides of the sample (K). Before being tested, specimens have been conditioned at  $T = 20^\circ\text{C}$  and RH = 50% until constant weight is reached (when the change in the weight of the test specimen over a 24 h period is less than 0.1%).

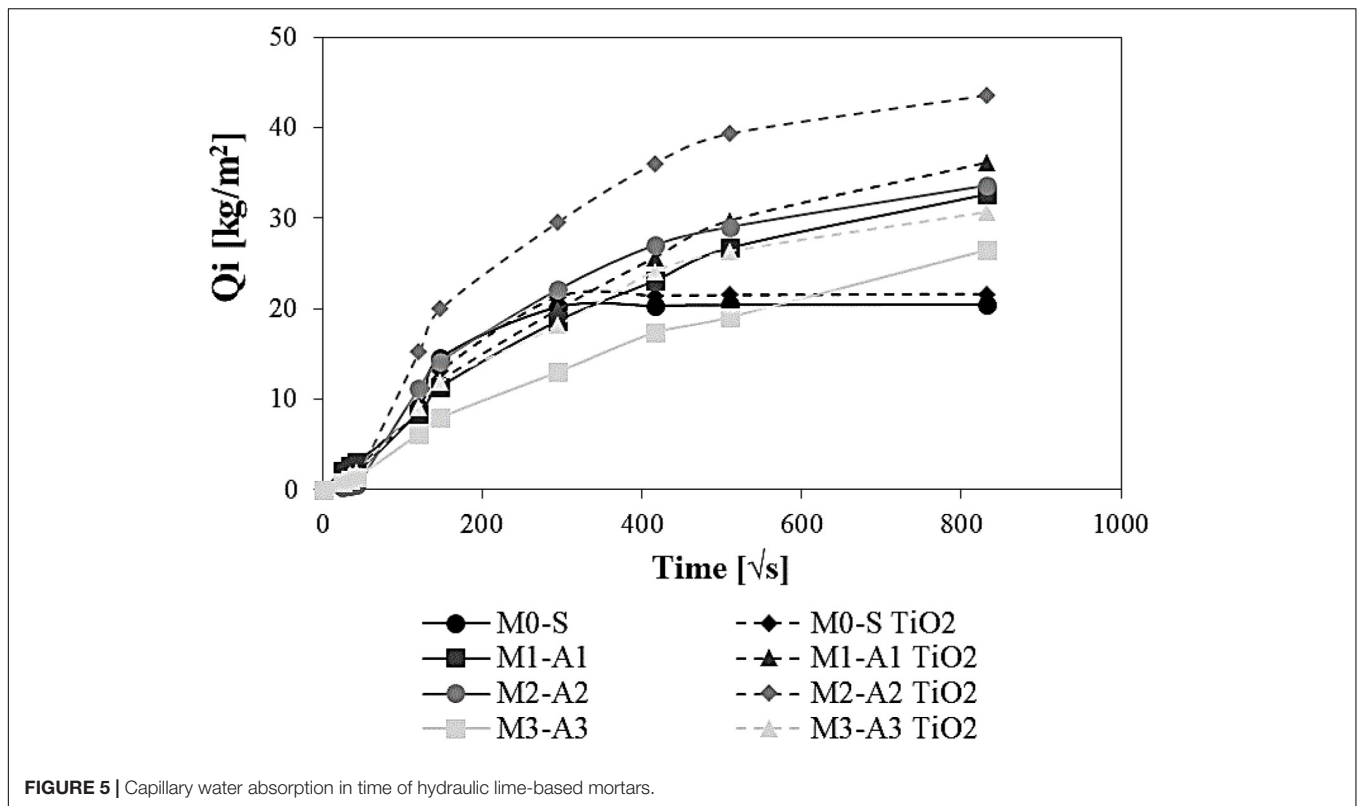
## RESULTS AND DISCUSSION

### Compressive Strength and Microstructural Observations

The compressive strength values already measured in Giosuè et al. (2020) and the morphological observations obtained by SEM are reported in **Figures 2, 3**. For the sake of brevity, in **Figure 3**, only images of specimens manufactured with different aggregates and TiO<sub>2</sub> are shown.

Since the main aim of this paper is to compare the effects of different types of aggregates on the ability of mortars to improve IAQ in terms of thermal conductivity and photocatalytic activity, the mixes are prepared by keeping constant both the water amount and the same water-to-binder ratio. For this fact, it is worth underlining that while the resulting compressing strength values for A2 mortars are good for applications as finishes/renders, those for A1 and A3 mortars are too high and not suitable for this type of application.

However, the good mechanical behavior of the mortar manufactured with sand (S) can be explained by the high mechanical strength of natural sand, due to its low porosity and the good adhesion between sand and hydraulic lime paste



(Figure 3a). EDAX analysis (Figure 4) evidences Ca of the aggregate and of the binder with Si and S present in the hydraulic-lime paste. TiO<sub>2</sub> particles are not visible in SEM images, confirming their optimum dispersion in the mix; anyhow, their presence is evident by EDAX analysis performed on the paste (Figure 4) due to the appearance of the Ti peak.

When the mortar is manufactured with zeolite (A1), even though zeolite is more porous, lighter, and therefore less resistant than natural sand, the mechanical resistance of the mortar remains high thanks to the pozzolanic activity of zeolite that forms additional hydration products, well visible as indicated in Figure 3b (Caputo et al., 2008; Uzal et al., 2010). Moreover, thanks to the pozzolanic reaction, the interfacial transition zone (ITZ) between zeolite and the binder paste can be hardly recognized, highlighting the optimum adhesion between the two components.

On the other hand, in Figure 3c, the ITZ between silica gel and hydraulic lime is clearly visible due to an evident detachment between the two components. As a matter of fact, the adhesion between hydraulic-lime paste and this type of aggregate appears very poor, due to the smooth surface of silica gel particles. This issue explains the worst mechanical behavior of silica gel-based mortars.

The ITZ between hydraulic lime paste and activated carbon is better than that with silica gel. In this case, even though activated carbon is more porous, lighter, and therefore less mechanical resistant than sand, the mechanical strength of mortars is even greater than that of sand-based mortars, probably thanks to its surface roughness which improves the adhesion with the

binder paste, guaranteeing an interlocking mechanism. This behavior was detected in other carbon-based materials with a porous surface that, acting as reservoirs, were able to provide a migration of water from their inside to the surrounding binder paste during the curing period, guaranteeing an optimum ITZ (Mrad and Chehab, 2019).

### Capillary Water Absorption

The open porosity is one of the most influencing parameters for water absorption of mortars: the higher the open porosity, the higher the water quantity that can fill the pores. Therefore, the use of unconventional aggregates increases the water uptake of mortars because they increase the porosity of the mortars compared to conventional sand (Giosuè et al., 2017b). As already demonstrated for these mixes (Giosuè et al., 2020) and reported in Table 2, the mortars with the highest value of open porosity are those manufactured with silica gel, followed by zeolite-based mortars and finally activated carbon-based mortars. The reference mortar has obviously the lowest porosity value.

In the absence of TiO<sub>2</sub>, as expected, the reference mortar, being the less porous, absorbs the lowest amount of water (Figure 5). Zeolite (A1)-based mortars adsorb an amount of water at 60%, higher than sand-based mortars. Silica gel (A2) mortars have the highest water absorption (80% higher than sand-based mortar) since they are the most porous.

Activated carbon-based mortars absorb lower (at the beginning of the test) and then higher (40%) amounts of water than sand-based mortars. This behavior is mainly related to the characteristics of the aggregate: activated carbon is hydrophobic

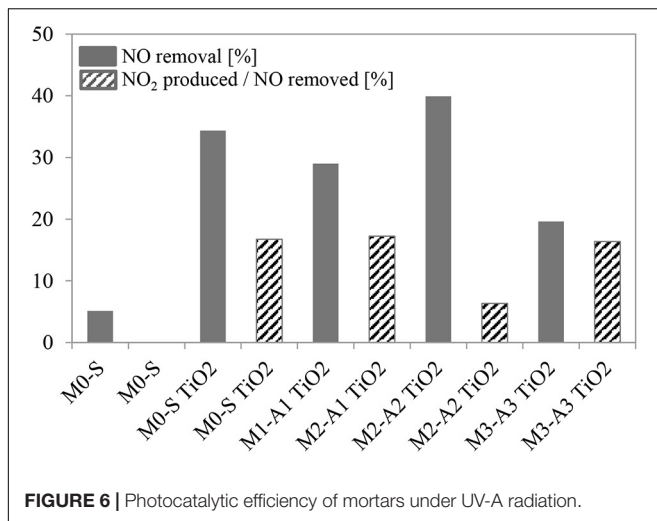


FIGURE 6 | Photocatalytic efficiency of mortars under UV-A radiation.

(Yang, 1987), with low affinity to water, at the early stage since it is a non-polar absorbent material, but it becomes hydrophilic for longer periods of contact with water and/or when some water has already been adsorbed (Giosuè et al., 2017b).

When the TiO<sub>2</sub> agent is added, generally the water absorption increases. This phenomenon, already shown in a previous study (Giosuè et al., 2017b), is due to the presence of TiO<sub>2</sub>, since the activation of the photocatalyst gives hydrophilicity to mortars (Banerjee et al., 2015; Zhang et al., 2015).

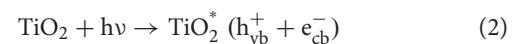
## Photocatalytic Oxidation

The behavior of mortars under photocatalytic radiation is reported in Figure 6. After the curing period, the pH of the specimens is evaluated as indicated in section “Methods.” After the cast, the pH value of the cementitious product is around 13.5 (Tittarelli et al., 2018). The results show that the finishes lose their initial strong basicity since the detected pH values are equal to 8 for all mortars, apart from those of the M3 series (M3-A3 and M3-A3 TiO<sub>2</sub>) with a pH of 8.5. For all TiO<sub>2</sub> specimens, a NO removal efficiency ranging from 20 to 40% is found. The lowest efficiency, equal to 20%, is registered in

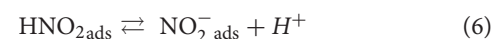
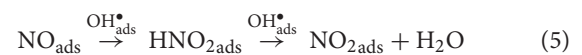
mortars manufactured with activated carbon; their dark color can reduce the reflectance of radiation and consequently influences the photocatalytic properties of the substrate (Chen and Poon, 2009; Daoud, 2013).

In the TiO<sub>2</sub>-mediated NO photocatalytic oxidation, NO<sub>2</sub> is produced as an unwanted product of the reaction. For this reason, the photocatalytic mortar exhibiting a lower NO<sub>2</sub> production should be preferred. In this regard, the ratio between NO<sub>2</sub> and NO is considered: the higher the ratio, the higher the production of unwanted NO<sub>2</sub> during the reaction (Pierpaoli et al., 2018). Whereas the ratio between the produced NO<sub>2</sub> and the removed NO is constant and around 16% for reference, zeolite, and activated carbon specimens, it is significantly lower when silica gel is used. This synergistic effect was already found in previous studies (Pierpaoli et al., 2018, 2019b) and may be attributed to an enhanced reactivity with the Ti-OH via NO<sub>2</sub> disproportionation (Eq. 9) caused by a more available adsorbed water in the vicinity of the photocatalyst (Dalton et al., 2002) and by the subsequent reaction of the nitrates with alkali or alkaline earth metals ions (Eq. 10).

TiO<sub>2</sub> photocatalysis



Oxidation via OH<sup>•</sup>



Oxidation via O<sub>2</sub><sup>-</sup>

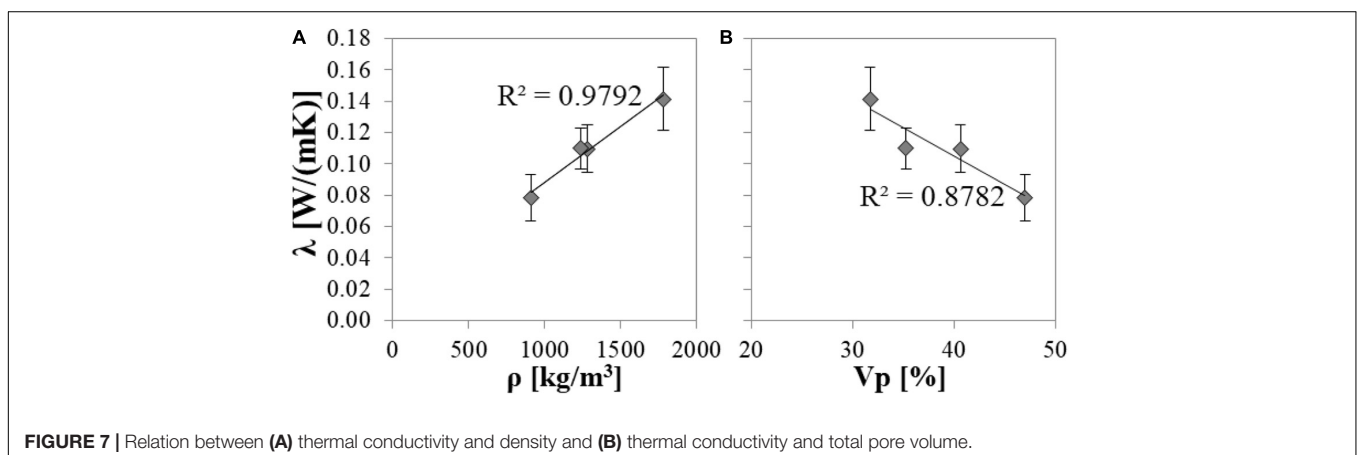
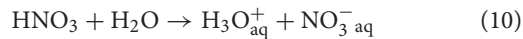


FIGURE 7 | Relation between (A) thermal conductivity and density and (B) thermal conductivity and total pore volume.

## Disproportionation of NO<sub>2</sub>



## Thermal Conductivity

The enhancement of the indoor comfort of occupants is strictly related to the thermal insulation of the environment: if building materials with low thermal conductivity are used, the thermal comfort can be guaranteed with a lower energy consumption by active systems. According to the standard UNI EN 998-1, the threshold limits for  $\lambda$  to classify a mortar as a T1 or T2 thermal mortar are 0.100 W/mK and 0.200 W/mK, respectively.

In the current study, almost all mortars can be classified as T2 mortar since their  $\lambda$  is lower than 0.200 W/mK. In particular, the reference mortar has the highest value ( $\lambda = 0.142$  W/mK), followed by activated carbon-based mortar and zeolite-based mortar with  $\lambda$  values of 0.110 and 0.110 W/mK, respectively. The lowest value of  $\lambda$  is detected in silica gel-based mortars (0.079 W/mK), which can be classified as a T1 mortar.

The  $\lambda$  of a mortar is related to both its density and porosity. The lower the density, the lower the thermal conductivity, and the higher the porosity, the lower the thermal conductivity (Demirboga and Gül, 2003). As expected, the use of highly porous aggregates permits to obtain lightweight mortars (Giosuè et al., 2018). Thanks to the total replacement of calcareous sand with silica gel (A2) and activated carbon (A3), lightweight finishes, highly appreciated for non-structural materials, can be obtained (Demirboga, 2003; Branco and Godinho, 2013).

Results of porosity and density of specimens are already shown in Giosuè et al. (2020), but in this paper the correlation between these properties and thermal conductivity is proposed and reported in **Figure 7**. Similar to the findings already published in other studies, a very good linear correlation between thermal conductivity and density (Coppola et al., 2018; Giosuè et al., 2019a) is obtained, as shown in **Figure 7A**. Usually, mortars with a high percentage of voids have strong insulating properties and can be used as plastering joints, building blocks, and panels able to guarantee the thermal comfort. Again, a linear correlation (but in this case with a lower coefficient) can be found between thermal conductivity and the total pore volume, as reported in **Figure 7B**.

## CONCLUSION

In the present work, hydraulic lime-based mortars manufactured with unconventional highly porous aggregates are studied to be used as multifunctional indoor finishes. Calcareous sand (S) is replaced entirely by volume with three different lightweight aggregates, namely, zeolite, silica gel, and activated carbon. Mortars are prepared with and without the addition of TiO<sub>2</sub>. The compressive strength values of these mortars are related to their microstructure observed by SEM. Then, the capillary water absorption, the photocatalytic oxidation of NO<sub>x</sub>, and the thermal conductivity are also investigated.

From the current research, it is possible to stand that:

- The dispersion of TiO<sub>2</sub> nanoparticles in the different analyzed matrixes is good, as shown by SEM analysis;
- Even though the mortars manufactured with lightweight aggregates have a lower density, the mechanical behavior of zeolite and activated carbon mortars is comparable or even higher than that of sand mortars, thanks to an optimum ITZ between the binder paste and the aggregate. In the case of silica gel-based mortars, the worst mechanical strength is due to the bad adhesion observed between this aggregate and the paste;
- Zeolite, silica gel, and activated carbon-based mortar adsorb a total amount of water 60%, 80%, and 40% higher than that of the reference mortar, respectively, because of their higher total porosity;
- The mortar prepared with silica gel exhibits the highest photocatalytic activity and the lowest selectivity toward NO<sub>2</sub> because of the higher availability of adsorbed water, which reflects into an enhanced production of OH radicals due to an enhanced reactivity with Ti-OH via disproportionation caused by a more available adsorbed water in the photocatalyst vicinity.
- An optimal linear correlation is confirmed between thermal conductivity and density, whereas a good linear correlation is found between porosity and density.

Further studies will be carried out in order to analyze the photocatalytic behavior of TiO<sub>2</sub> active under visible light.

## Permission to Reuse and Copyright

Figures, tables, and images will be published under a Creative Commons CC-BY license, and permission must be obtained for use of copyrighted material from other sources (including republished/adapted/modified/partial figures and images from the internet). It is the responsibility of the authors to acquire the licenses, to follow any citation instructions requested by third-party rights holders, and to cover any supplementary charges.

## DATA AVAILABILITY STATEMENT

The raw data supporting the conclusions of this article will be made available by the authors, without undue reservation.

## AUTHOR CONTRIBUTIONS

CG: original research plan, methodology and investigation, material characterization, specimen preparation, original manuscript draft, and preliminary data curation. MP: collaboration in data curation of photocatalytic activities and manuscript editing. AM: collaboration in data curation of thermal conductivity, and manuscript review and editing. FT: coordination and supervision of the project, analysis of data, and manuscript draft and editing. MR: supervision of tests to evaluate the depolluting properties of mortars, interpretation of relative data, and manuscript editing. All authors contributed to the article and approved the submitted version.



## REFERENCES

- Ballari, M. M., Yu, Q. L., and Brouwers, H. J. H. (2011). Experimental study of the NO and NO<sub>2</sub> degradation by photocatalytically active concrete. *Catal. Today* 161, 175–180. doi: 10.1016/j.cattod.2010.09.028
- Banerjee, S., Dionysiou, D. D., and Pillai, S. C. (2015). Self-cleaning applications of TiO<sub>2</sub> by photo-induced hydrophilicity and photocatalysis. *Appl. Catal. B Environ.* 17, 396–428. doi: 10.1016/j.apcatb.2015.03.058
- Barcelo, L., Kline, J., Walenta, G., and Gartner, E. (2013). Cement and carbon emissions. *Mater. Struct.* 47, 1055–1065. doi: 10.1617/s11527-013-0114-5
- Benfratello, S., Capitano, C., Peri, G., Rizzo, G., Scaccianoce, G., and Sorrentino, G. (2013). Thermal and structural properties of a hemp-lime biocomposite. *Constr. Build Mater.* 48, 745–754. doi: 10.1016/j.conbuildmat.2013.07.096
- Branco, F. G., and Godinho, L. (2013). On the use of lightweight mortars for the minimization of impact sound transmission. *Constr. Build Mater.* 45, 184–191. doi: 10.1016/j.conbuildmat.2013.04.001
- Caputo, D., Liguori, B., and Colella, C. (2008). Some advances in understanding the pozzolanic activity of zeolites: the effect of zeolite structure. *Cem. Concr. Compos.* 30, 455–462. doi: 10.1016/j.cemconcomp.2007.08.004
- Chen, J., and Poon, C. S. (2009). Photocatalytic activity of titanium dioxide modified concrete materials – Influence of utilizing recycled glass cullets as aggregates. *J. Environ. Manage.* 90, 3436–3442. doi: 10.1016/j.jenvman.2009.05.029
- Coppola, B., Courard, L., Michel, F., Incarnato, L., Scarfato, P., and Di, L. (2018). Hygro-thermal and durability properties of a lightweight mortar made with foamed plastic waste aggregates. *Constr. Build Mater.* 170, 200–206. doi: 10.1016/j.conbuildmat.2018.03.083
- Dalton, J. S., Janes, P. A., Jones, N. G., Nicholson, J. A., Hallam, K. R., and Allen, G. C. (2002). Photocatalytic oxidation of NO<sub>x</sub> gases using TiO<sub>2</sub>: a surface spectroscopic approach. *Environ. Pollut.* 120, 415–422. doi: 10.1016/s0269-7491(02)00107-0
- Daoud, W. A. (2013). *Self-Cleaning Materials and Surfaces A Nanotechnology Approach*. Chichester: John Wiley & Sons.
- Demirboga, R. (2003). Influence of mineral admixtures on thermal conductivity and compressive strength of mortar. *Energy Build.* 35, 189–192. doi: 10.1016/s0378-7788(02)00052-x
- Demirboga, R., and Gül, R. (2003). Thermal conductivity and compressive strength of expanded perlite aggregate concrete with mineral admixtures. *Energy Build.* 35, 1155–1159. doi: 10.1016/j.enbuild.2003.09.002
- Folli, A., Pade, C., Hansen, T. B., De Marco, T., and Macphee, D. E. (2012). TiO<sub>2</sub> photocatalysis in cementitious systems: insights into self-cleaning and depollution chemistry. *Cem. Concr. Res.* 42, 539–548. doi: 10.1016/j.cemconres.2011.12.001
- Frey, S. E., Destaillets, H., Cohn, S., Ahrentzen, S., and Fraser, M. P. (2015). The effects of an energy efficiency retrofit on indoor air quality. *Indoor Air.* 25, 210–219. doi: 10.1111/ina.12134
- Giosuè, C., Belli, A., Mobili, A., Citterio, B., Biavasco, F., Ruello, M. L., et al. (2017a). Improving the impact of commercial paint on indoor air quality by using highly porous fillers. *Buildings* 7:110. doi: 10.3390/buildings7040110
- Giosuè, C., Mobili, A., Citterio, B., Biavasco, F., Ruello, M. L., and Tittarelli, F. (2020). Innovative hydraulic lime-based finishes with unconventional aggregates and TiO<sub>2</sub> for the improvement of indoor air quality. *Manuf. Rev.* 7, 1–9.
- Giosuè, C., Mobili, A., Di, C., and Tittarelli, F. (2019a). Performance of lightweight cement-based and alkali-activated mortars exposed to high-temperature. *Constr. Build Mater.* 220, 565–576. doi: 10.1016/j.conbuildmat.2019.05.193
- Giosuè, C., Mobili, A., Yu, Q. L., Brouwers, H. J. H., Ruello, M. L., and Tittarelli, F. (2019b). Properties of multifunctional lightweight mortars containing zeolite and natural fibers. *J. Sustain. Cem. Mater.* 8, 214–217.
- Giosuè, C., Pierpaoli, M., Mobili, A., Ruello, M. L., and Tittarelli, F. (2017b). Influence of binders and lightweight aggregates on the properties of cementitious mortars: from traditional requirements to indoor air quality improvement. *Materials* 10:978. doi: 10.3390/ma10080978
- Giosuè, C., Yu, Q. L., Ruello, M. L., Tittarelli, F., and Brouwers, H. J. H. (2018). Effect of pore structure on the performance of photocatalytic lightweight lime-based finishing mortar. *Constr. Build Mater.* 171, 232–242. doi: 10.1016/j.conbuildmat.2018.03.106
- Han, B., Wang, Y., Dong, S., and Zhang, L. (2016). Smart concretes and structures: a review. *J. Intell. Mater. Syst. Struct.* 26, 1303–1345. doi: 10.1177/1045389x15586452
- Horgnies, M., Dubois-Brugger, I., and Gartner, E. M. (2012). NO<sub>x</sub> de-pollution by hardened concrete and the influence of activated charcoal additions. *Cem. Concr. Res.* 42, 1348–1355. doi: 10.1016/j.cemconres.2012.06.007
- Kaja, A. M., Brouwers, H. J. H., and Yu, Q. L. (2019). NO<sub>x</sub> degradation by photocatalytic mortars: the underlying role of the CH and C-S-H carbonation. *Cem Concr Res.* 125:105805. doi: 10.1016/j.cemconres.2019.10.5805
- Karatasiou, I., Katsiotis, M. S., Likodimos, V., Kontos, A. I., Papavassiliou, G., Falaras, P., et al. (2010). Photo-induced carbonation of lime-TiO<sub>2</sub> mortars. *Appl. Catal. B Environ.* 95, 78–86. doi: 10.1016/j.apcatb.2009.12.011
- Lucas, S. S., Ferreira, V. M., and Aguiar, J. L. B. (2013). Incorporation of titanium dioxide nanoparticles in mortars — Influence of microstructure in the hardened state properties and photocatalytic activity. *Cem. Concr. Res.* 43, 112–120. doi: 10.1016/j.cemconres.2012.09.007
- MacPhee, D. E., and Folli, A. (2016). Photocatalytic concretes - The interface between photocatalysis and cement chemistry. *Cem Concr Res.* 85, 48–54. doi: 10.1016/j.cemconres.2016.03.007
- Masel, R. I. (1996). *Principles of Adsorption and Reaction on Solid*. New York, NY: John Wiley & Sons, 818.
- Matsumoto, H., Shimizu, M., and Sato, H. (2009). The contaminant removal efficiency of an air cleaner using the adsorption/desorption effect. *Build Environ.* 44, 1371–1377. doi: 10.1016/j.buildenv.2008.09.006
- Mrad, R., and Chehab, G. (2019). Mechanical and microstructure properties of biochar-based mortar: an internal curing agent for PCC. *Sustainability* 11:2491. doi: 10.3390/su11092491
- Pierpaoli, M., Fava, G., and Ruello, M. L. (2019a). Electroadsorptive removal of gaseous pollutants. *Appl. Sci.* 9:1162. doi: 10.3390/app9061162
- Pierpaoli, M., Favoni, O., Fava, G., and Ruello, M. L. (2018). A novel method for the combined photocatalytic activity determination and bandgap estimation. *Methods Protoc.* 1, 1–12.
- Pierpaoli, M., Giosuè, C., Ruello, M. L., and Fava, G. (2017). Appraisal of a hybrid air cleaning process. *Environ. Sci. Pollut. Res.* 24, 12638–12645. doi: 10.1007/s11356-016-7880-x
- Pierpaoli, M., and Ruello, M. L. (2018). Indoor air quality: a bibliometric study. *Sustainability* 10:3830. doi: 10.3390/su10113830
- Pierpaoli, M., Zheng, X., Bondarenko, V., Fava, G., and Ruello, M. L. (2019b). Paving the path to a sustainable and efficient SiO<sub>2</sub> / TiO<sub>2</sub> photocatalytic composite. *Environments* 6:87. doi: 10.3390/environments6080087
- Senff, L., Ascensão, G., Ferreira, V. M., Seabra, M. P., and Labrincha, J. A. (2018). Development of multifunctional plaster using nano-TiO<sub>2</sub> and distinct particle size cellulose fibers. *Energy Build.* 158, 721–735. doi: 10.1016/j.enbuild.2017.10.060
- Senff, L., Tobaldi, D. M., Lucas, S., Hotza, D., Ferreira, V. M., and Labrincha, J. A. (2013). Formulation of mortars with nano-SiO<sub>2</sub> and nano-TiO<sub>2</sub> for degradation of pollutants in buildings. *Compos Part B.* 44, 40–47. doi: 10.1016/j.compositesb.2012.07.022
- Sugrañez, R., Álvarez, J. I., Cruz-yusta, M., Mármol, I., Morales, J., Vila, J., et al. (2013). Enhanced photocatalytic degradation of NO<sub>x</sub> gases by regulating the microstructure of mortar cement modified with titanium dioxide. *Build. Environ.* 69, 55–63. doi: 10.1016/j.buildenv.2013.07.014
- Tittarelli, F., Giosuè, C., Mobili, A., and Ruello, M. L. (2015). Influence of binders and aggregates on VOCs adsorption and moisture buffering activity of mortars for indoor applications. *Cem. Concr. Compos.* 57, 75–83. doi: 10.1016/j.cemconcomp.2014.11.013
- Tittarelli, F., Mobili, A., Giosuè, C., Belli, A., and Bellezze, T. (2018). Corrosion behaviour of bare and galvanized steel in geopolymer and Ordinary Portland Cement based mortars with the same strength class exposed to chlorides. *Corros Sci.* 134, 64–77. doi: 10.1016/j.corsci.2018.02.014
- Trník, A., Fo, J., Pavlíková, M., Pokorn, J., and Cern, R. (2016). Modified lime-cement plasters with enhanced thermal and hygric storage capacity for moderation of interior climate. *Energy Build.* 126, 113–127. doi: 10.1016/j.enbuild.2016.05.004
- Uzal, B., Turanlı, L., Yücel, H., Göncüoğlu, M. C., and Çulfaz, A. (2010). Pozzolanic activity of clinoptilolite: a comparative study with silica fume, fly ash and a

- non-zeolitic natural pozzolan. *Cem. Concr. Res.* 40, 398–404. doi: 10.1016/j.cemconres.2009.10.016
- Wang, S., Yan, C., and Xiao, F. (2012). Quantitative energy performance assessment methods for existing buildings. *Energy Build.* 55, 873–888. doi: 10.1016/j.enbuild.2012.08.037
- Washburn, E. W. (1921). Note on a method of determining the distribution of pore sizes in a porous material. *Proc. Natl. Acad. Sci. U. S. A.* 7, 115–116. doi: 10.1073/pnas.7.4.115
- Wolkoff, P. (2013). Indoor air pollutants in office environments: assessment of comfort, health, and performance. *Int. J. Hyg. Environ. Health.* 216, 371–394. doi: 10.1016/j.ijheh.2012.08.001
- Yang, R. (1987). *Gas Separation by Adsorption Processes*. Oxford: Butterworth Publisher.
- Yu, Q. L., Spiesz, P., and Brouwers, H. J. H. (2015). Ultra-lightweight concrete: conceptual design and performance evaluation. *Cem. Concr. Compos.* 61, 18–28. doi: 10.1016/j.cemconcomp.2015.04.012
- Zhang, R., Cheng, X., Hou, P., and Ye, Z. (2015). Influences of nano-TiO<sub>2</sub> on the properties of cement-based materials: hydration and drying shrinkage. *Constr. Build Mater.* 81, 35–41. doi: 10.1016/j.conbuildmat.2015.02.003

**Conflict of Interest:** The authors declare that the research was conducted in the absence of any commercial or financial relationships that could be construed as a potential conflict of interest.

Copyright © 2020 Giosuè, Pierpaoli, Mobili, Ruello and Tittarelli. This is an open-access article distributed under the terms of the Creative Commons Attribution License (CC BY). The use, distribution or reproduction in other forums is permitted, provided the original author(s) and the copyright owner(s) are credited and that the original publication in this journal is cited, in accordance with accepted academic practice. No use, distribution or reproduction is permitted which does not comply with these terms.